FIG. 5.1

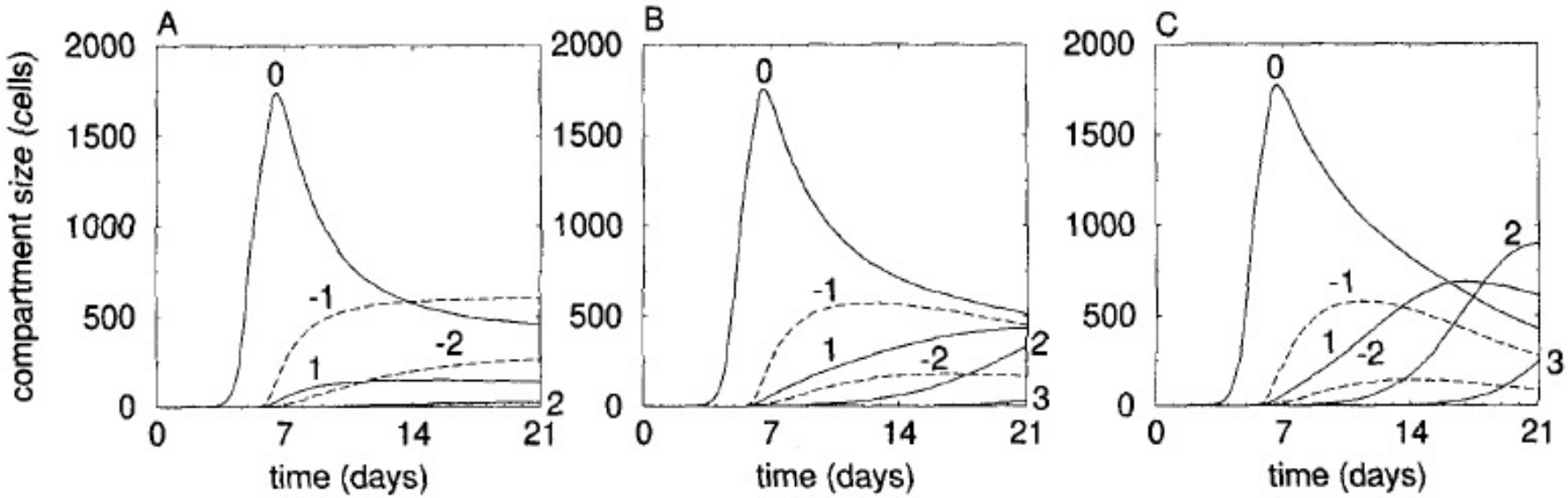

FIG. 5.1: The evolution of B cells in different affinity classes predicted by Perelson's model of GC processes. Affinity class 0 corresponds to germline B cells, vells in classes -1 and -2 have increasingly worse affinity compared to germline B cells, and those in classes 1, 2, and 3 have increasingly better affinities. Panels A, B, and C correspond to results for the fraction of recycled positively selected B cells equal to 0.1, 0.5, and 0.9. High affinity B cells only emerge if the fraction recycled is high.

FIG. 5.2

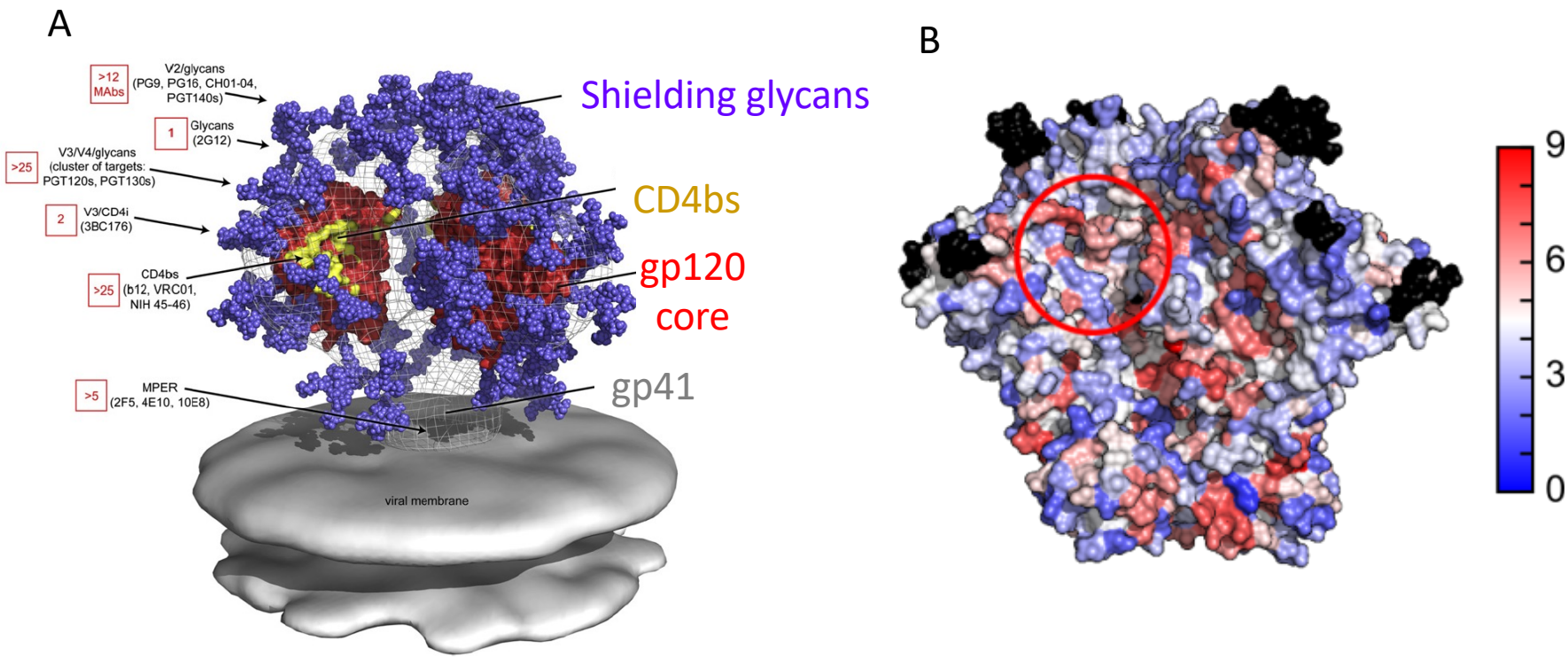

FIG. 5.2: (A) Schematic depiction of the viral spike of HIV. The yellow region corresponds to the relatively conserved CD4 binding site that is targeted by bnAbs that have been isolated from patients. Some other relatively conserved epitopes that are targeted by known bnAbs are also indicated. The red region is highly variable, and the blue residues represent glycans that can shield the spike protein residues from antibodies. (B) The fitness cost of evolving mutations at a particular residue averaged over for all possible amino acids at that residue in all possible sequence backgrounds (see Chapter 5) is shown superimposed on a representation of the HIV spike trimer. The region surrounding the CD4 binding site is circled in red. Bluer colors indicate lower fitness costs associated with mutations.

C

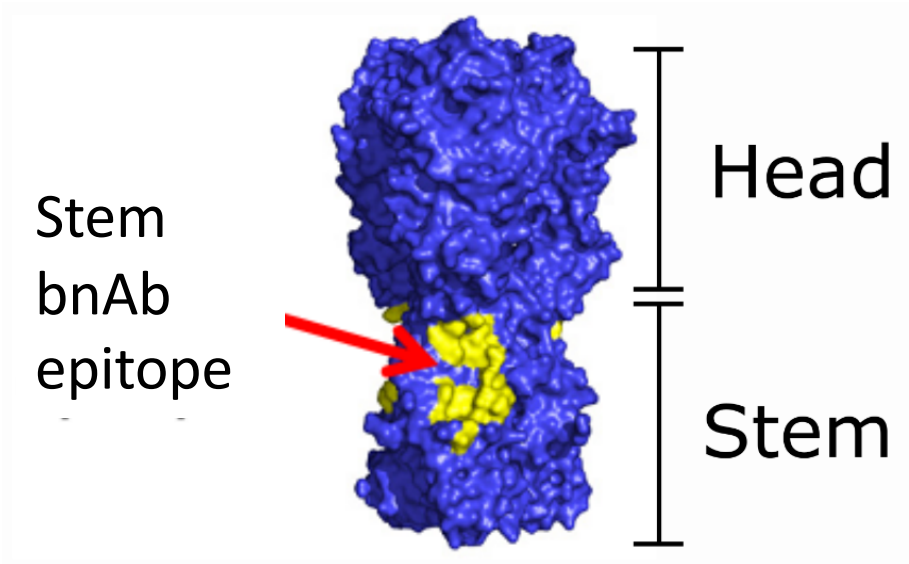

(C) Schematic representation of the HA spike on the surface of the influenza virus. The sonserved stem epitope is shown in yellow. The conserved residue of the RBS are not shown.

Fig. 5.3

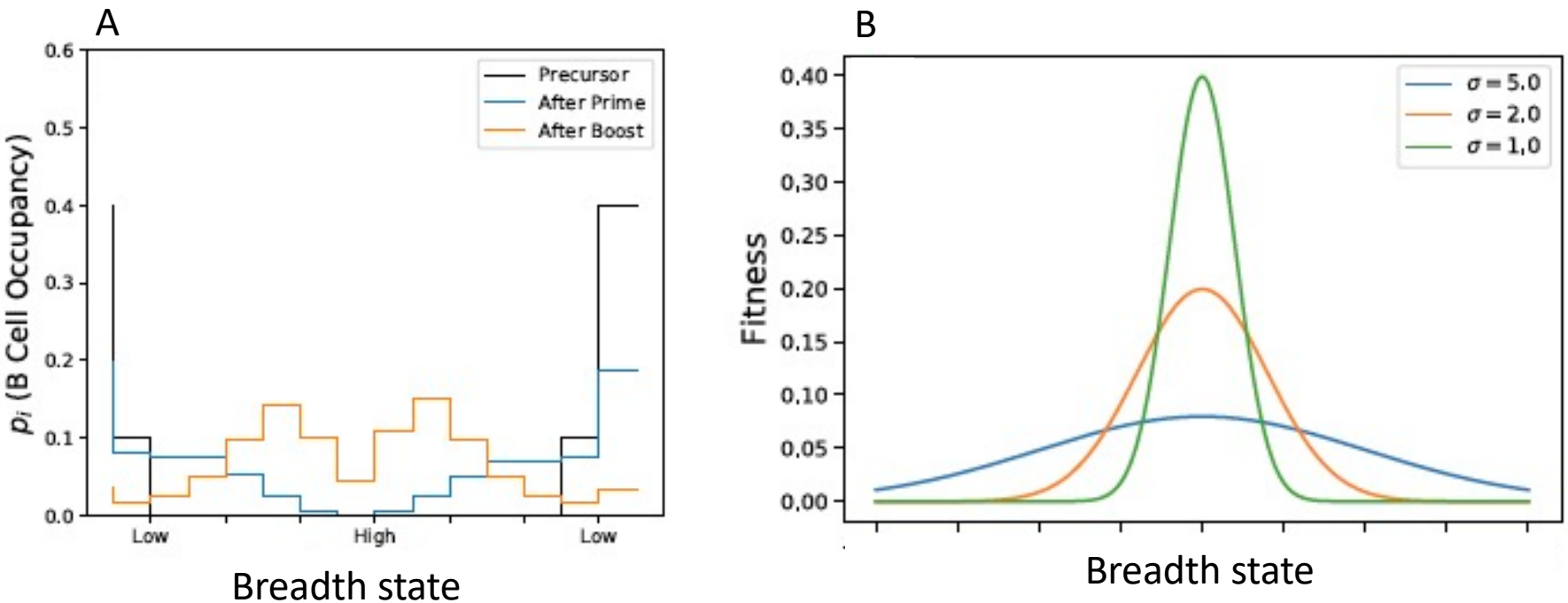

Fig. 5.3: A one-dimensional projection of BCR/antibody sequence defined in a higher-dimensional space is assumed to define the breadth of a B cell. The state at the center of the axis representing breadth corresponds to the highest breadth, and edges correspond to the lowest. (A) Schematic depiction of the probability distribution of B cells in different breadth states: B cells that seed GCs (black line), after a first immunization or prime (blue line), and after a second immunization or boost (orange line). (B) Schematic depictions of the probability of B cells of different breadth being positively selected per unit time (or "fitness"). The probability distributions depicted correspond to Gaussian distributions with different values of the variance (σ)

Fig. 5.4

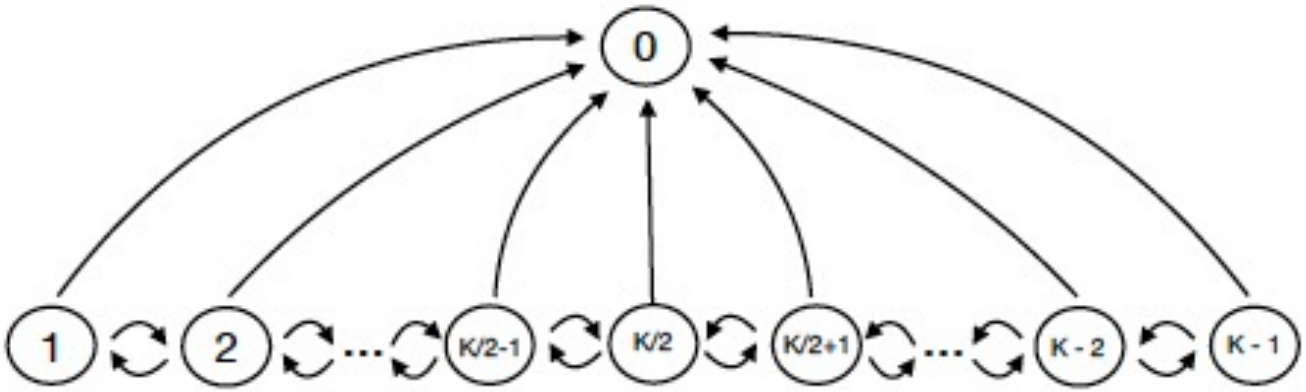

Fig. 5.4: Discrete representation of breadth states. The K/2th bin (middle bin) is the highest breadth state, and bin 1 and bin K-1 represent the lowest breadth states. Bin 0 corresponds to dead B cells (absorbing state). B cells can transition between breadth states by mutation, and transitions to the dead state occur either due to lethal mutations or a basal death rate.

Fig. 5.5

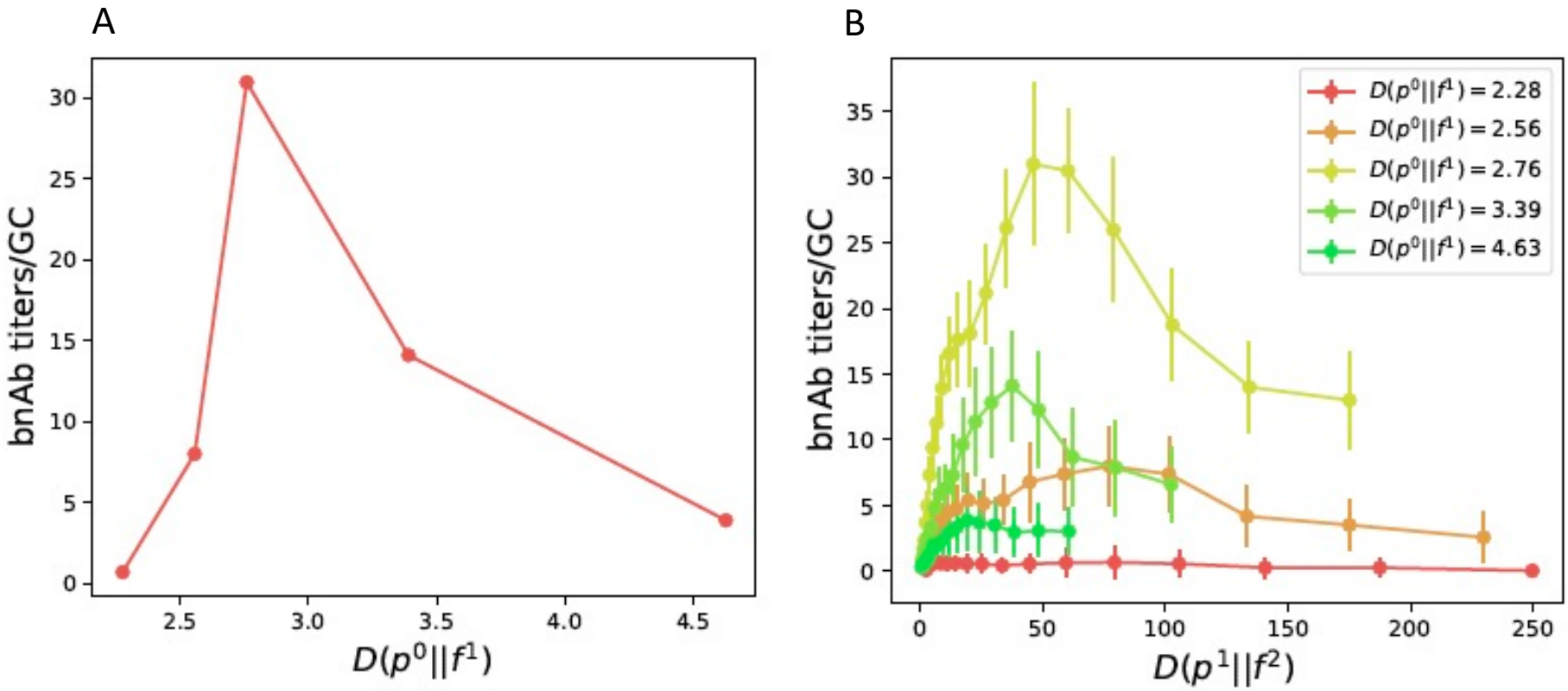

Fig. 5.5: (A) The number (titers) of bnAbs/GC after the first immunization is shown as a function of the KLD ($D(p^0||f^1)$) between the initial B cell population and the fitness distribution imposed by the immunogens in the first immunization. (B) For each value of $D(p^0||f^1)$, the number (titers) of bnAbs/GC is shown as a function of the KLD ($D(p^1||f^2)$) between the B cell distribution produced after the first immunization and the fitness distribution imposed by the immunogens in the second immunization.

Fig. 5.6

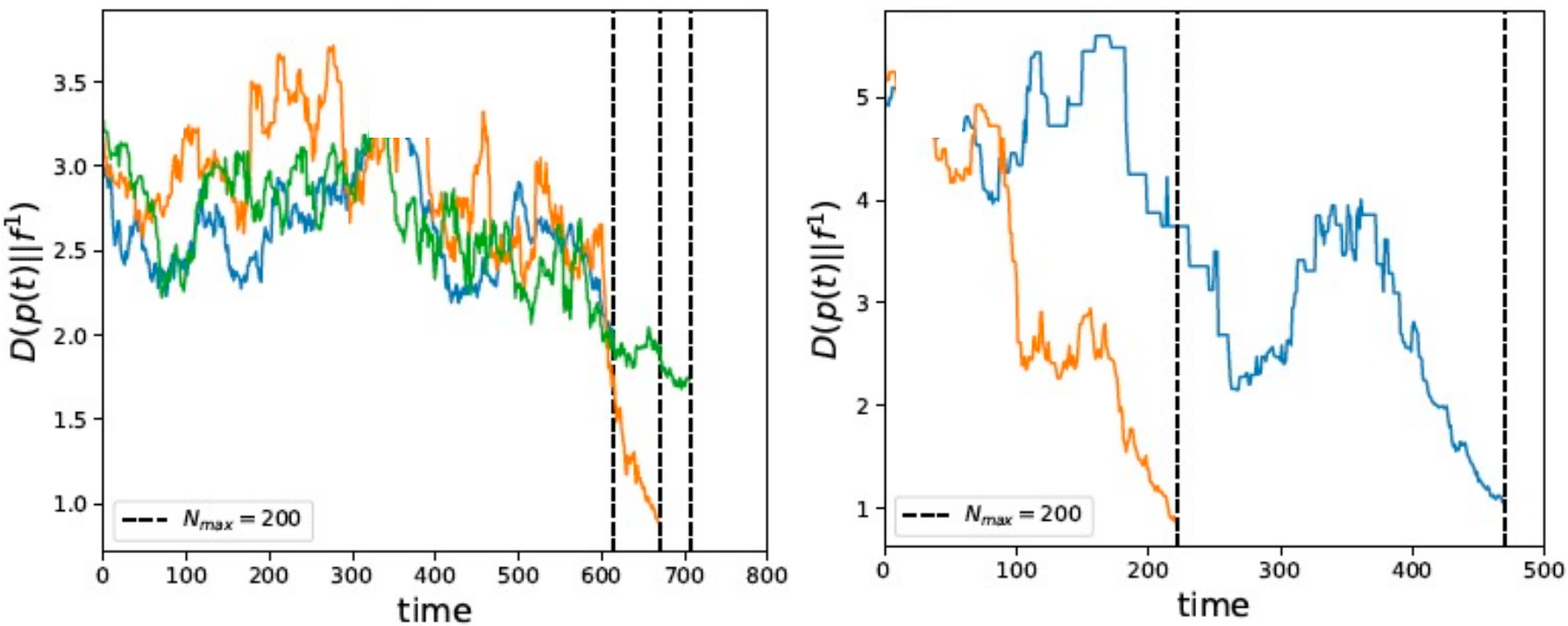

Fig. 5.6: The GC B cells adapt to their environment as time ensues, and so evolutionary trajectories show that the KLD between the distribution of GC B cells at time t, p (t), and the fitness distribution imposed by the first immunization (D $(p(t)||f^1)$) decreases with time. (A) Three examples of trajectories for D $(p^0||f^1) = 3.15$ are shown. (B) Two examples of trajectories for D $(p^0||f^1) = 5.16$ are shown.

Fig. 5.7

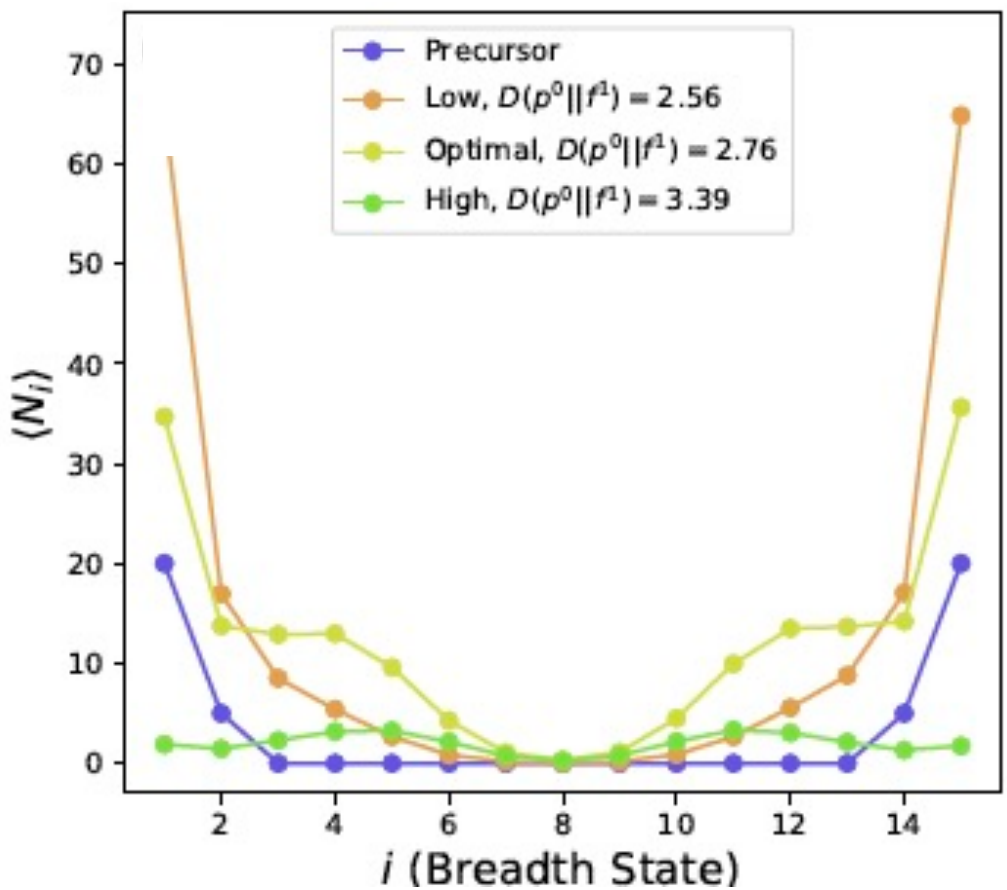

Fig. 5.7: The average number of B cells, $\langle N_i \rangle$, in each breadth state, i, of the precursor B cells that seed GCs, and after the first immunization for different values of the KLD, D ($p^0||f^1$). For low values of the KLD, after immunization, most B cells occupy states of low breadth, and for large values of the KLD, most GC B cells die and the B cell population is very small. For the optimal value of the KLD, after the first immunization, B cells occupy states with relatively high breadth with reasonable probability.

Fig. 5.8

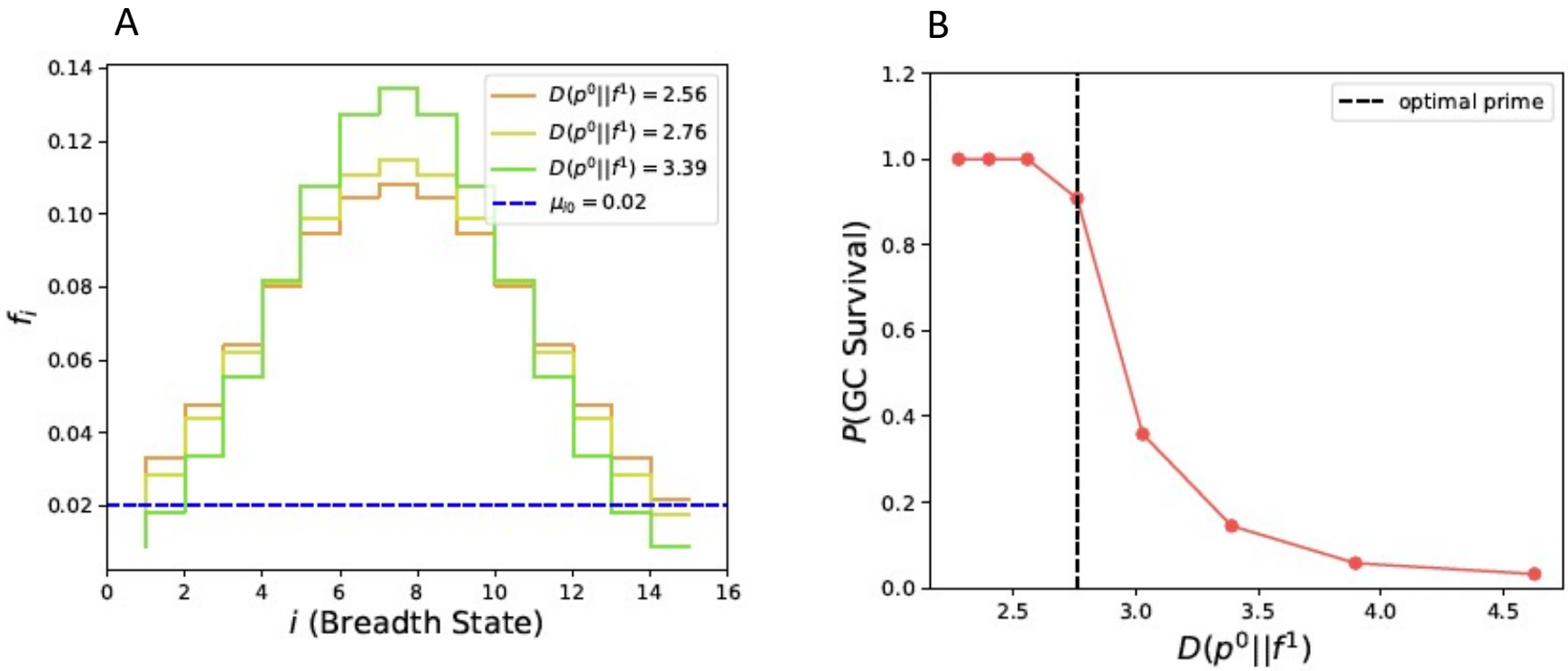

Fig. 5.8: (A) The probability of being positively selected per unit time (f_i) corresponding to various values of D ($p^0||f^1$). The curve for the optimal value of D ($p^0||f^1$) = 2.76 goes below the basal death rate at the edge states. If D ($p^0||f^1$) is higher (e.g., 3.39), the value of f_i goes below the basal death rate for states with higher breadth. (B)The fraction of GCs that do not go extinct, P (GC Survival) is shown as a function of D ($p^0||f^1$). The value of D ($p^0||f^1$) corresponding to the optimal prime is shown as the vertical dashed line.

Fig. 5.9

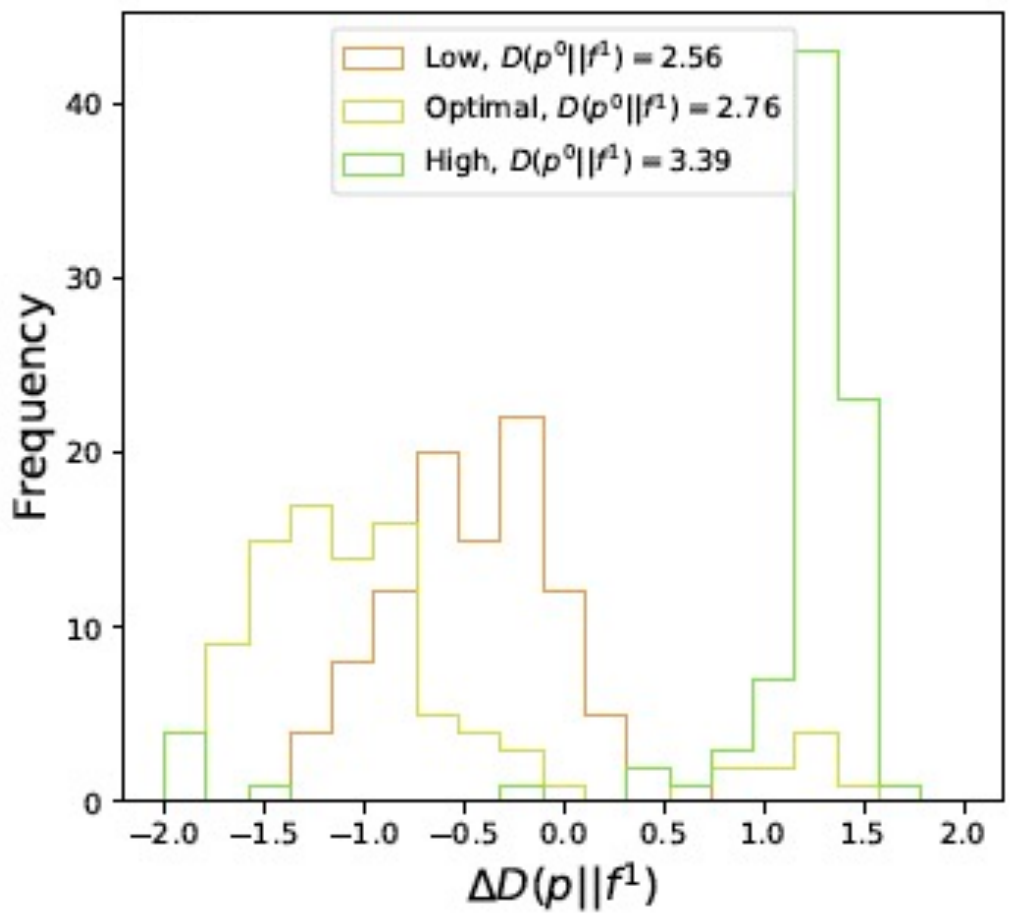

Fig. 5.9: For low (brown), optimal (yellow), and high (green) values of D ($p^0||f^1$), the change in D after GC reactions, $\Delta D\ (p||f^1)$, is recorded for each simulated GC and the results are shown as a histogram. More negative values of $\Delta D\ (p||f^1)$ correspond to better adaptation of the B cell population to the immunogen, which is the desired response to vaccination.

Fig. 5.10

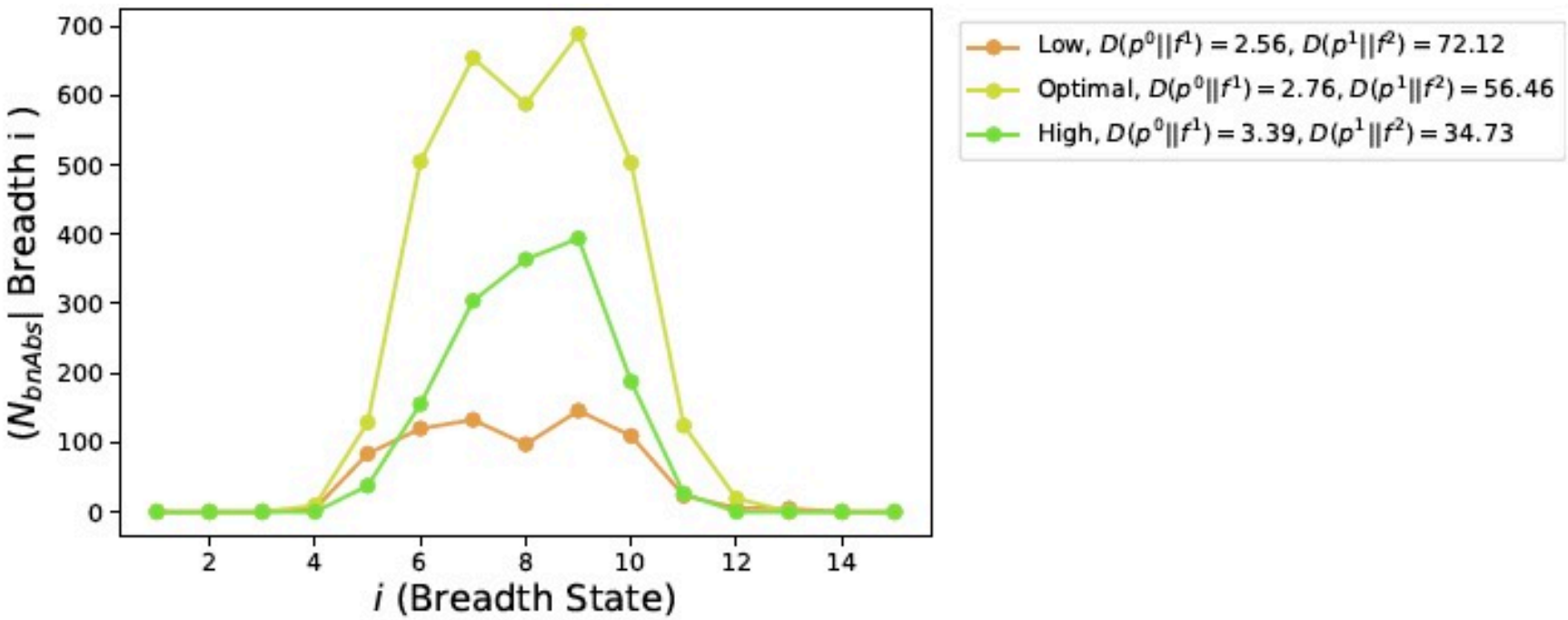

Fig. 5.10: The number of evolutionary trajectories that result in bnAbs (N_{bnAbs}) originating from B cells in different breadth states, i, after prime. Examples of low and high values of D ($p^0||f^1$), and the optimal value are shown. For each value of D ($p^0||f^1$), the boost immunogen corresponds to the optimal value of D ($p^1||f^2$).

Fig. 5.11

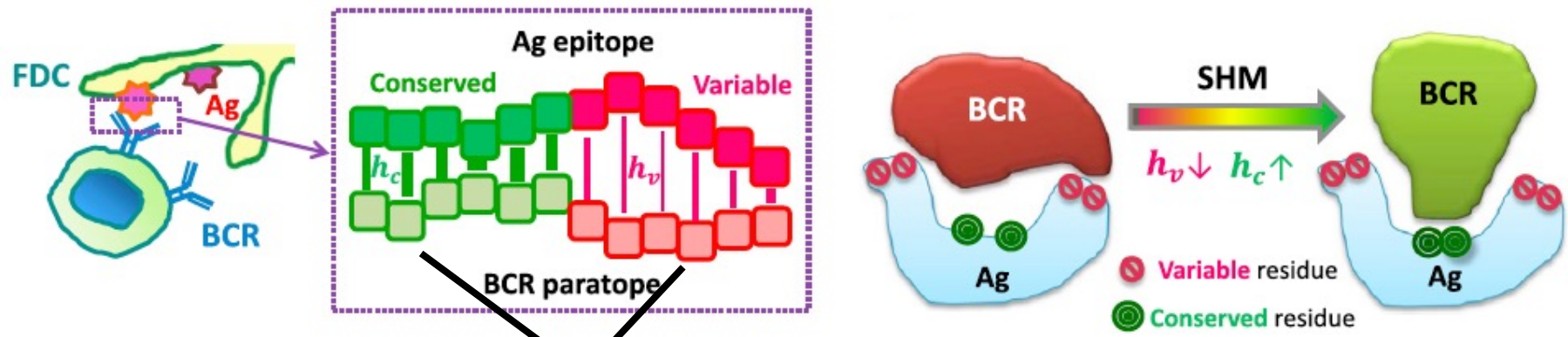

$$E_{ij} = \sum_{k=1}^{M} h_k^i \, s_k^j + \sum_{k=M+1}^{N} h_k^i .$$

IF $|h_k'| < |h_k|$

$$-\alpha(|h_k'| - |h_k|) > 0$$

Fig. 5.12

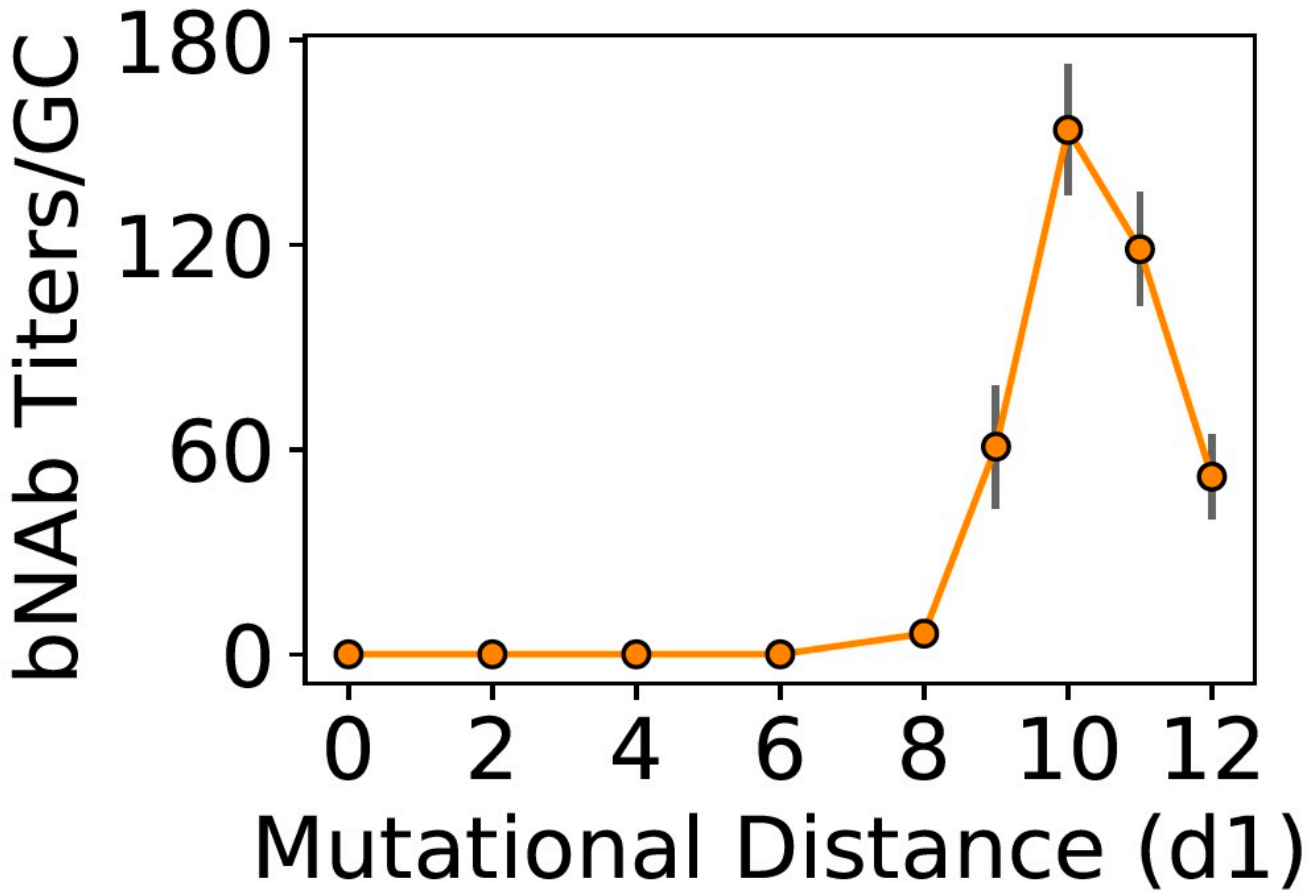

Fig. 5.12: The number (titers) of bnAbs/GC is shown as a function of the mutational distance between the first immunogen and the GL targeting antigen, d1 (see text) at a fixed value of the immunogen concentration. The maximum is analogous to the maximum shown in Fig. 5.5 A.

Fig. 5.13

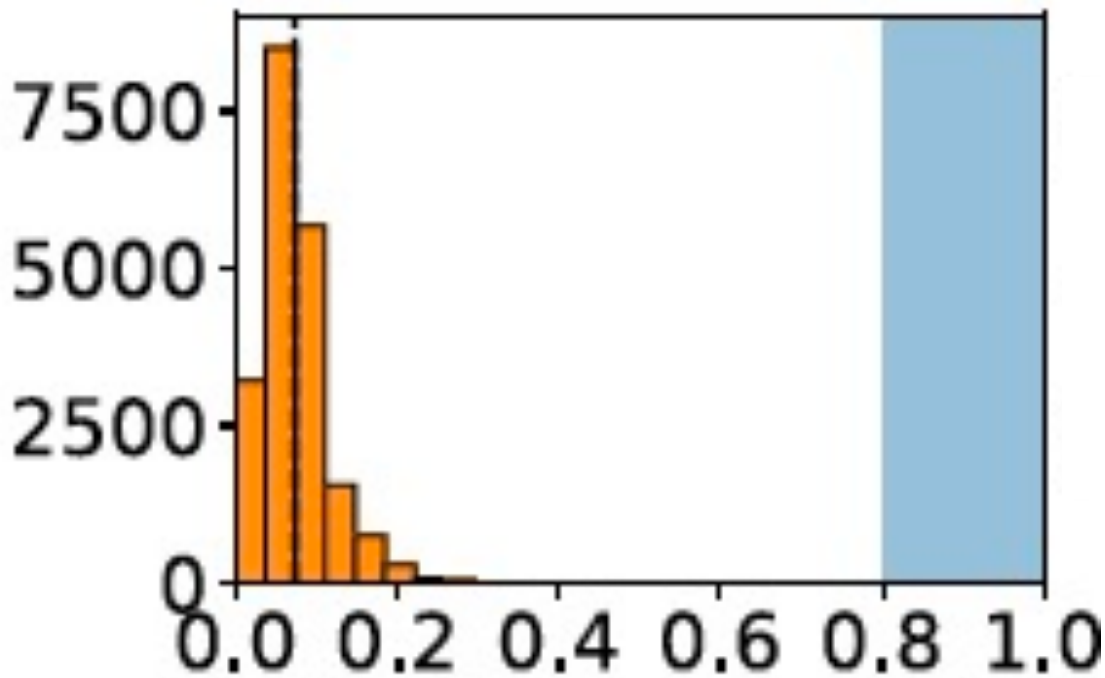

Fig. 5.13: A histogram showing the distribution of breadths of the antibodies produced upon the first immunization when the mutational distance separating the first immunogen and the GL targeting antigen is small (d = 4 in Fig. 5.12). The blue shaded region corresponds to bnAbs.

Fig. 5.14

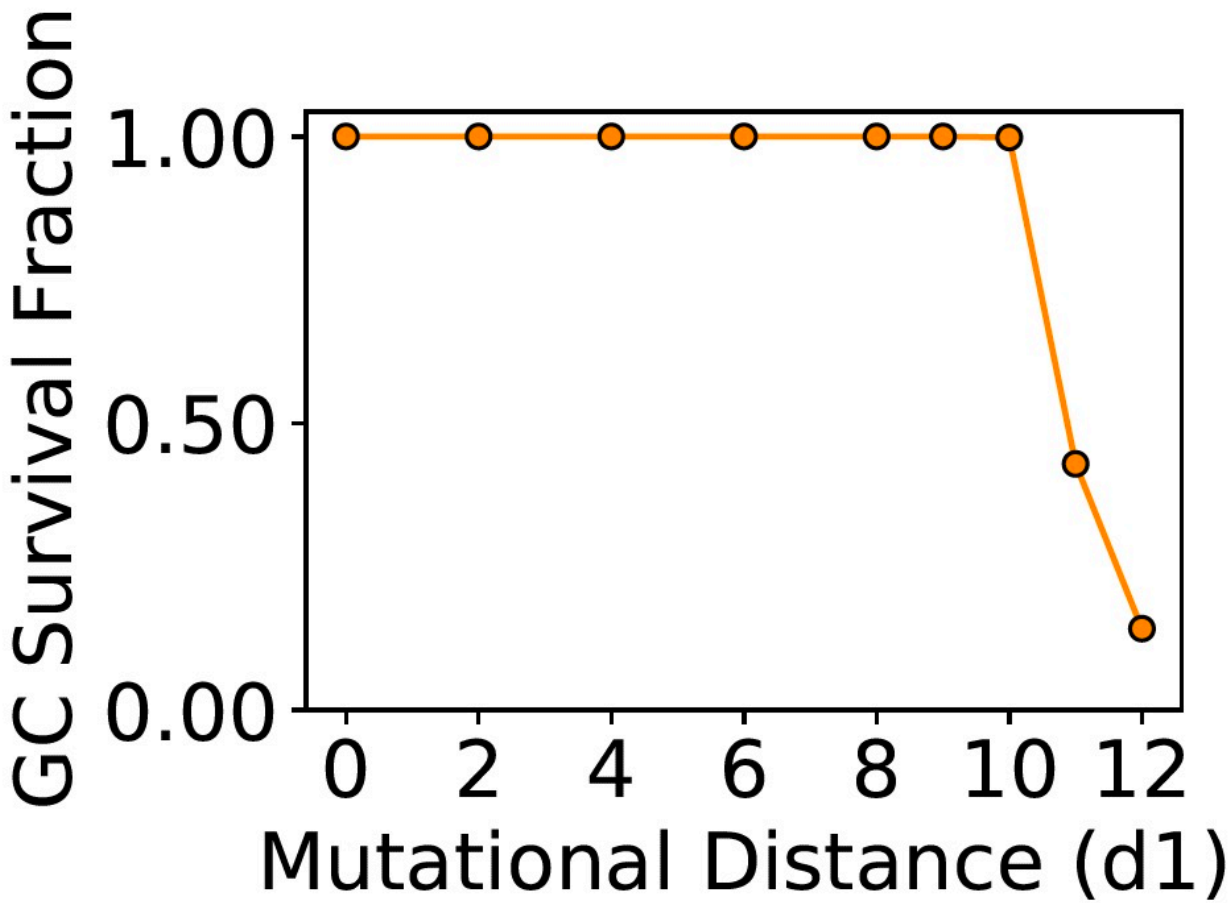

Fig. 5.14: The GC survival rate goes down dramatically around the optimal value of the mutational distance for the first immunogen. This behavior is analogous to that shown in Fig. 5.8 B using the simple one-dimensional model. All simulation conditions are identical to that corresponding to the results shown in Fig. 5.12.

Fig. 5.15

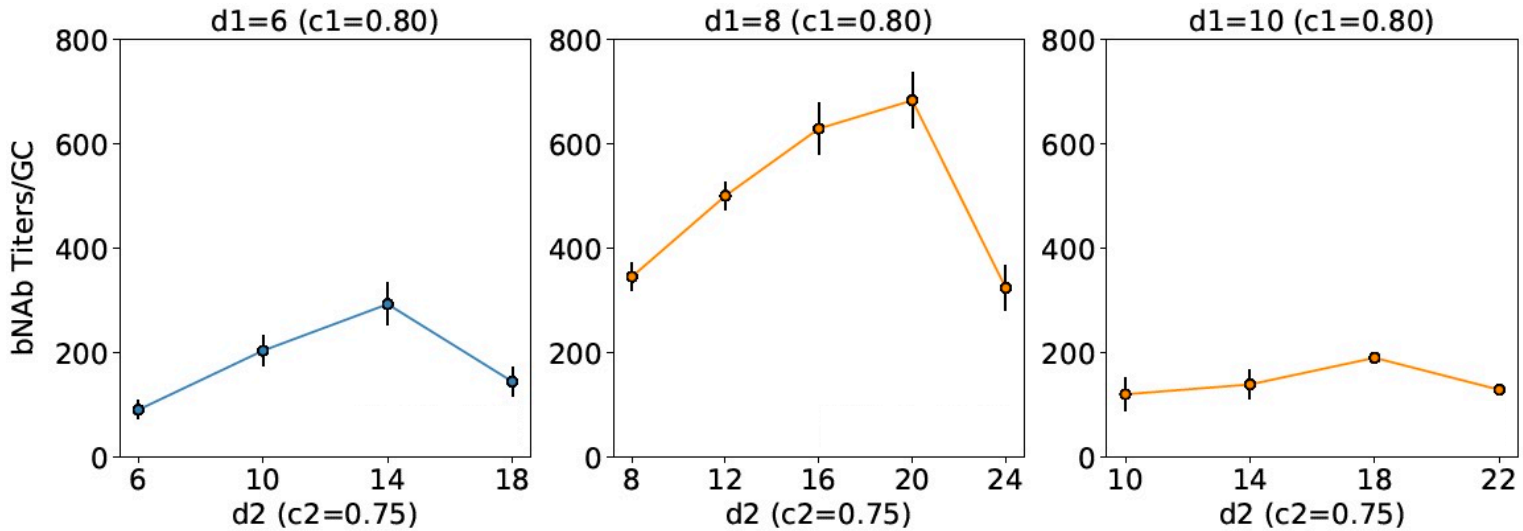

Fig. 5.15: The bnAb titers/GC after the second immunization graphed against the mutational distance (d_2) between the second and first immunogens for three different values of the mutational difference between the first immunogen and the GL targeting antigen (d_1). The antigen concentrations, c1 and c2, for the two immunizations, respectively are also noted.

Fig. 5.16

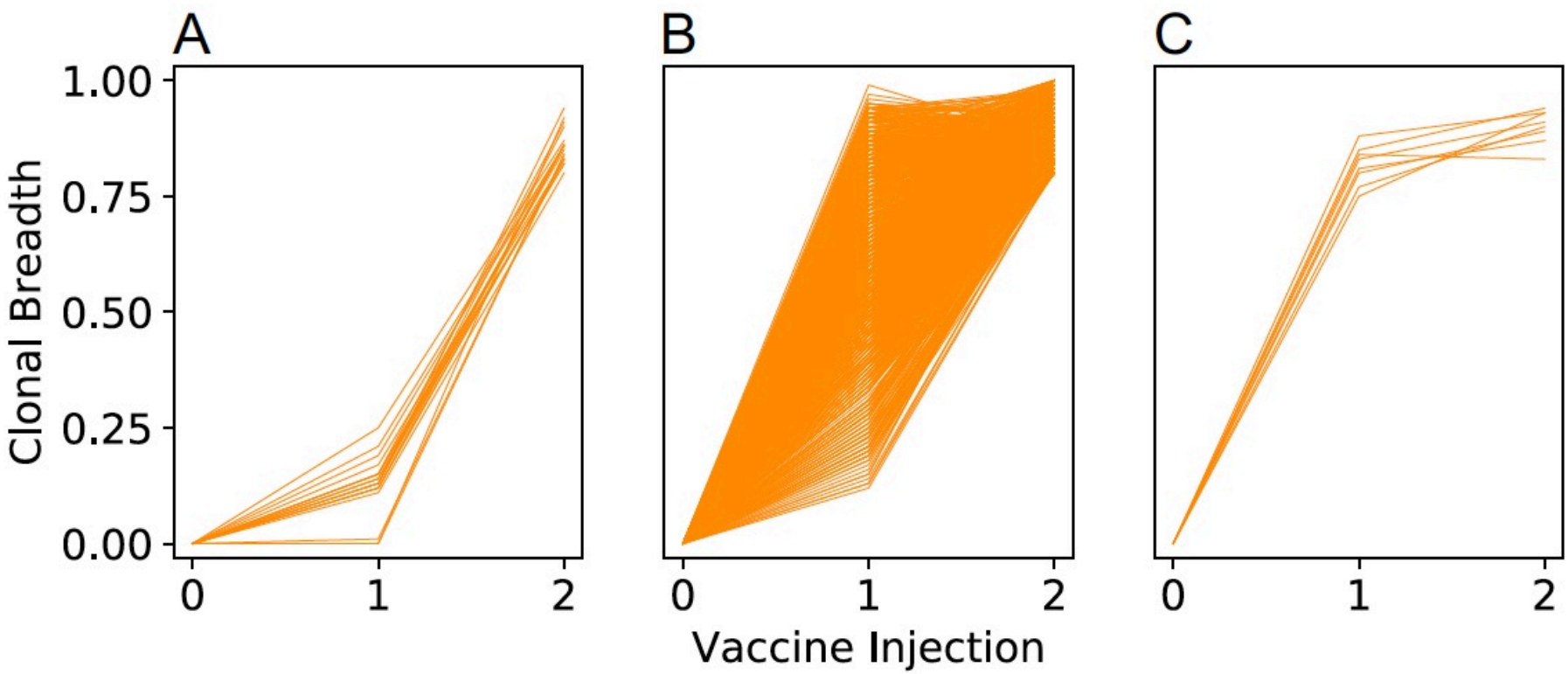

Fig. 5.16: The number of evolutionary trajectories that lead to bnAbs. The abscissa levels 1 and 2 correspond to the first and second immunizations, respectively. Results for high (A), optimal (B), and low (C) antigen concentration during the first immunization are shown. The mutational distance, d_1 ($d_{Ag1\text{-}GL}$) is equal to 4, and d_2 ($d_{Ag1\text{-}Ag2}$+$d_{Ag2\text{-}GL}$) is equal to 8.

Fig. 5.17

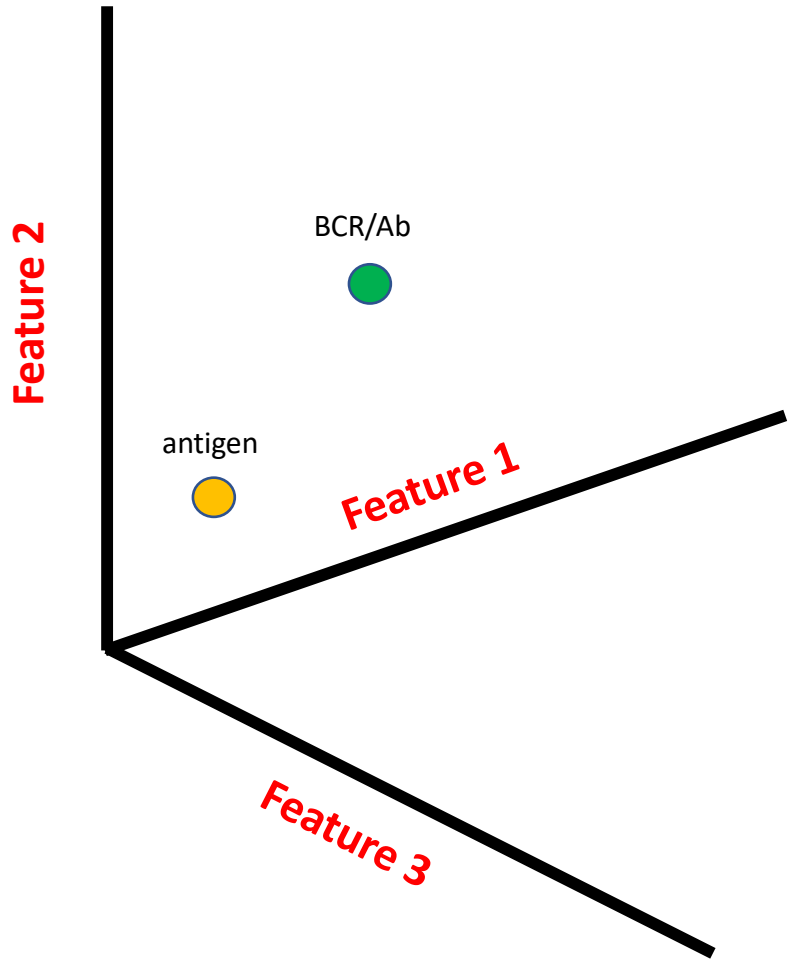

Fig. 5.17: A schematic depiction of "shape space" for the free energy of interaction between a BCR/antibody and an antigen. Each axes corresponds to a particular feature (e.g., charge, hydrophobicity, conformation, etc) of the BCR/antibody and the complementary feature of the antigen. A particular BCR/antibody or an antigen is thus represented as a point in this shape space. For simplicity, a 3-dimensional shape space is shown.

Fig. 5.18

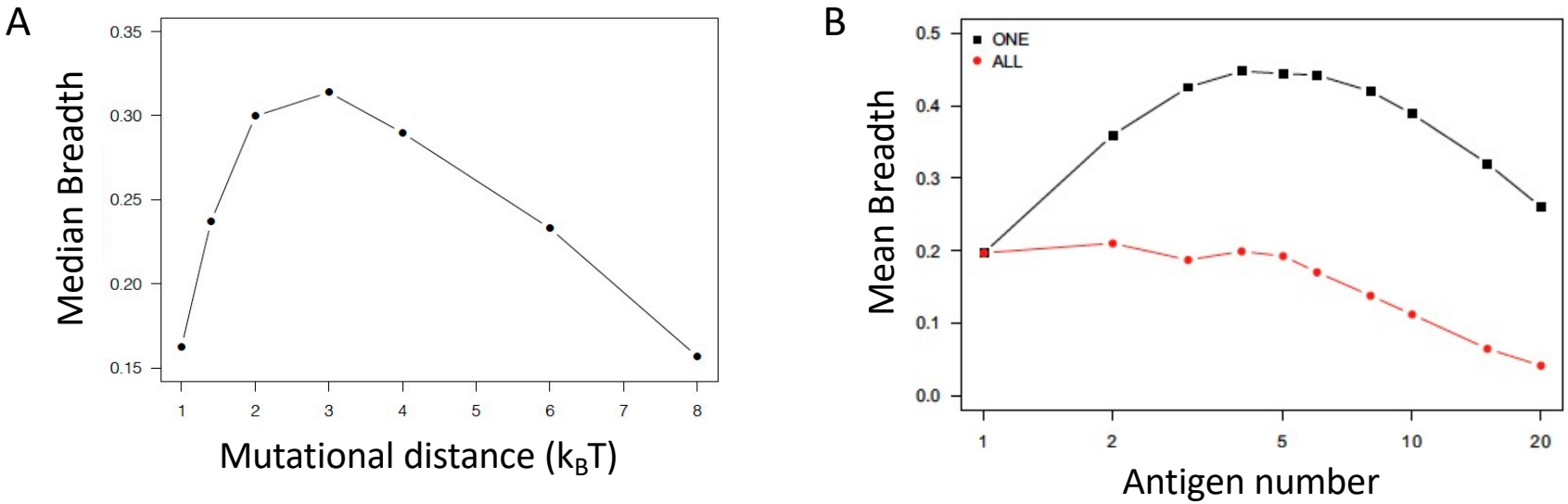

Fig. 5.18: Optimal cocktails of variant antigens maximize the breadth of antibodies.(A) The median breadth of antibodies produced upon immunization with a cocktail of variant antigens whose variable regions are separated by different mutational distances. The mutational distances are specified in units of k_BT as per Eq. 15. The number of antigens is 5, and the antigen concentration is 20 (units as per Eq. 19). (B) The mean breadth of antibodies produced as a function of the number of variant antigens. The mutational distance between the antigens is 2 k_BT , and c = 0.2. A comparison between the cases when only one variant antigen is encountered in every round of selection and all are encountered is also shown.

Fig. 5.19

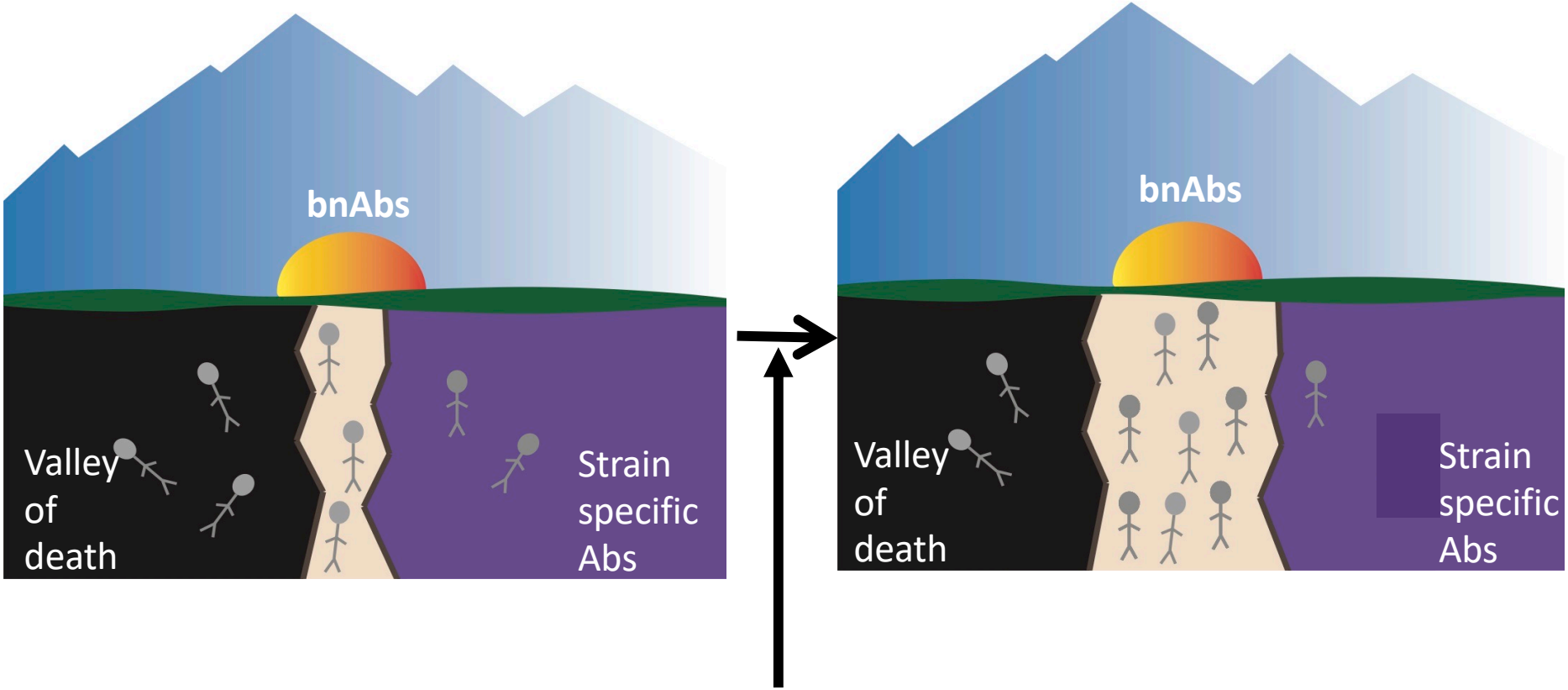

There are optimal sequential immunization strategies that maximize bnAb evolution

Fig. 5.19: A schematic representation of the challenge associated with maximizing the evolution of bnAbs.

Fig. 5.20

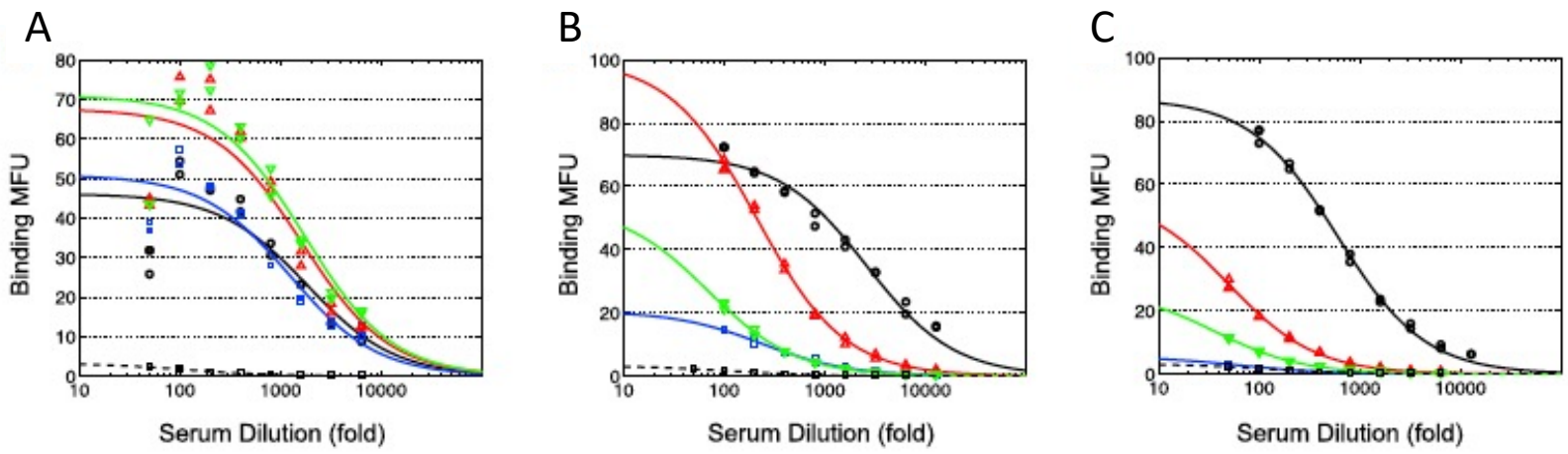

Fig. 5.20: Two groups of mice were immunized with four variant immunogens composed of a modified form of the monomer of GP120. The ability of the generated antibodies to bind to each of the four variant antigens (black, red, green and blue curves) is shown. The abscissa corresponds to the extent to which serum taken from mice is diluted; smaller values correspond to a higher concentration of antibodies. The ordinate is a measure of the amount of bound antibodies measured using a fluorescence assay; MFU corresponds to mean fluorescent units. Data from representative immunized mice are shown. The black dashed line corresponds to serum taken from a mouse that was not immunized. (A) Sequential immunization. (B) Immunization with a cocktail of the same variant immunogens. (C) Immunization with one of the variant immunogens.

Fig. 5.21

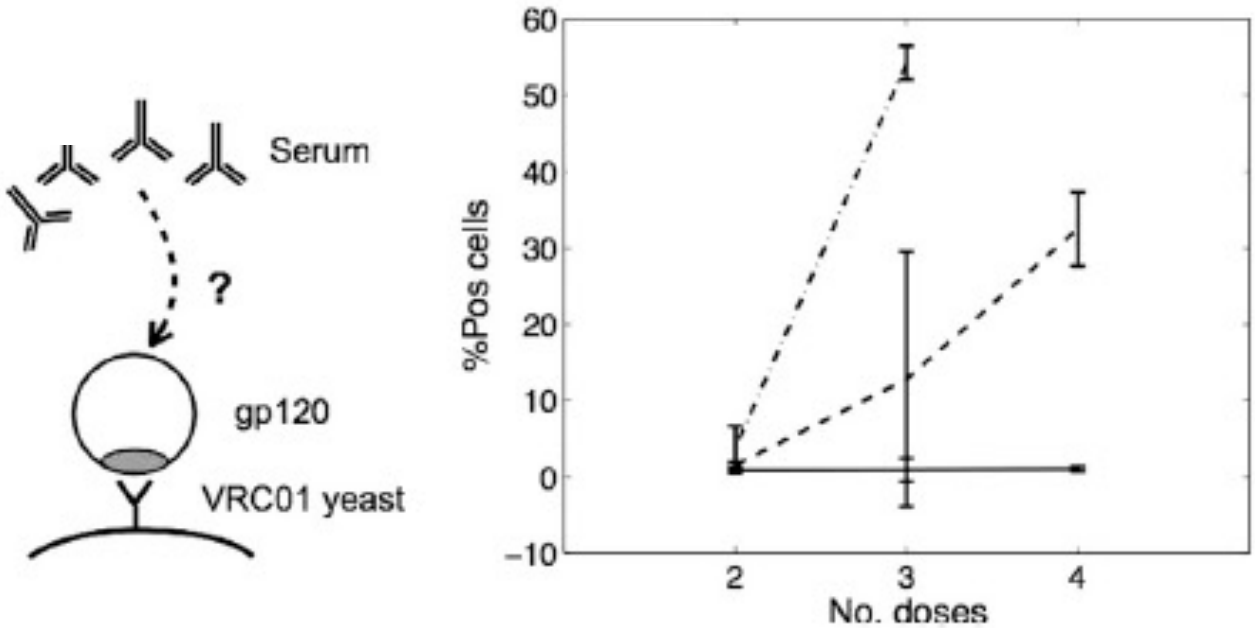

Fig. 5.21: VRCO1, a HIV bnAb that binds to the CD4 binding site of gp 120 (shown as shaded area in left panel) was displayed on the surface of yeast. The gp 120 antigen was then added, followed by serum antibodies. The percentage of serum antibodies that bound is shown in the right panel for sera taken from mice immunized sequentially with variant antigens (solid line), antigen cocktail (dashed line), and a single antigen (dot dashed line). The data show results obtained by following the same mice across multiple immunizations. The error bars reflect the standard deviation across mice that were immunized using the same immunization protocol. Due to technical details of the assay, 60 % positive cells is the maximum signal that can be observed.

TABLE 1

For the edge states $i = 1$ and $i = 15$,

$$N_1 \xrightarrow{f_1} 2\,N_1$$

$$N_1 \xrightarrow{\mu_{1,2}} N_2$$

$$N_1 \xrightarrow{\mu_{1,0}} N_0$$

$$N_{15} \xrightarrow{f_{15}} 2\,N_{15}$$

$$N_{15} \xrightarrow{\mu_{15,14}} N_{14}$$

$$N_{15} \xrightarrow{\mu_{15,0}} N_0$$

For all states between $i = 1$ and $i = 15$,

$$N_i \xrightarrow{f_i} 2\,N_i$$

$$N_i \xrightarrow{\mu_{i,i-1}} N_{i-1}$$

$$N_i \xrightarrow{\mu_{i,i+1}} N_{i+1}$$

$$N_i \xrightarrow{\mu_{i,0}} N_0$$